Journal of İstanbul Kültür University
2006/4 pp.77-89

MODELING THE NONLINEAR BEHAVIOUR OF A DRIVEN VARACTOR RESONATOR AT LOW FREQUENCIES

John A. KALOMIROS[1], Stavros G. STAVRINIDES[1], Amalia N. MILIOU[2], Mehmet OZER[3], Taner BULAT[3]

Abstract

We monitor the theoretical response of an R-L-Varactor circuit by using Multisim 7.0, at a driving frequency *f=1MHz* with high driving amplitudes. At low frequencies a bifurcation is observed, attributed to the large capacitance emerging from the carrier injection at reverse-bias breakdown. By increasing driving amplitude we observe non-periodic trajectories with increasing chaotic content in a four dimensional state-space. At specific amplitudes we monitor two-dimensional tori where trajectories are periodic, like in a two-oscillators system with commensurate frequencies. The scenario from quasi-periodocity to chaos is discussed by means of established tools, like the circle map, Poincare cross sections, power and FFT spectra, correlation dimension and Kolmogorov entropy. Peak amplitudes of the monitored waveforms are shown to form an interesting pattern of well defined groups, within the resolution of the numerical solutions produced by the simulation.

I. Introduction

One of the best known simple circuits that produce a wealth of chaotic phenomena is the oscillator formed by a resistor inductor and a varactor diode connected in series (fig. 1). It is a non-autonomous passive circuit that displays bifurcation and chaos, with control parameters the sinusoidal driving frequency and amplitude. Different bifurcation diagrams can be obtained by changing the inductance or the type of the varactor or by varying the value of the damping resistor. Many publications report on such phenomena while a number

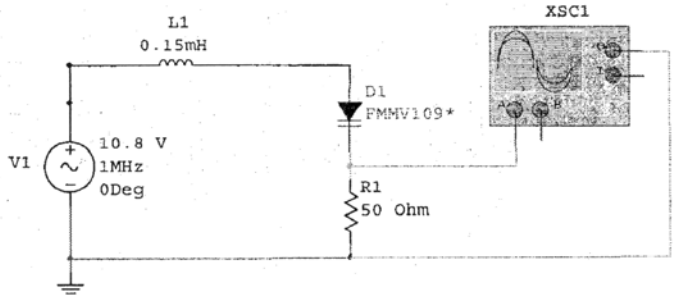

Figure 1: *R-L-Varactor in series studied by Multisim program*

of articles analyze the possible sources of bifurcation and chaos [1-7], in the high frequency range. The role of nonlinear capacitance of the varactor diode [4,5] and the contribution of finite reverse recovery time to nonlinearity [3,8,9] are discussed in a major body of the relative literature.

[1] *J.A.Kalomiros and S.G.Stavrinides are with the Physics Department, Aristotle University of Thessaloniki, GR-54124 Thessaloniki, Greece.*
[2] *A.N.Milou is with the Department of Informatics, Aristotle University of Thessaloniki, GR54124 Thessaloniki, Greece.*
[3] *M.Ozer and T.Bulat are with the Physics Department, Istanbul Kultur University, Istanbul, Turkey.*

In this article we use a combination of the electronic circuits simulator Multisim 7.0 and the digital processing and data acquisition software LabView 7.1 as a tool to further probe and research nonlinear behavior in the RLD circuit.

It is well established that chaotic dynamics is easily observed for driving frequencies in the vicinity and above the resonant frequency $f_0=1/[2\pi(LC_0)^{1/2}]$, where C_0 is the zero bias capacitance of the varactor. In our circuit of fig. 1 this resonant frequency is $f_0=1,6MHz$.

In this report we focus on the sub-resonance region where low amplitude signals do not present complex dynamic. However using a driving frequency of 1MHz, well below the resonant frequency and amplitudes from 1V to 17V, simulation results suggest a new resonance effect for high driving amplitudes.

The components used in the simulation were a FMMV109 Si diode varactore, a resistor R=50 Ohms and an inductor L=150μH. This circuit was studied experimentally by Klinker et al. [6] at frequencies above 1MHz and with low driving amplitudes. We should note that our theoretical simulation reproduces fairly well most of the observations by Klinger et al. above the resonance frequency.

II. Simulated response in the sub-resonance region

The control parameter in our study is the amplitude of the external signal, fig. 1. At relatively low amplitudes (1-10 Volts) the output signal measured on the external resistor R is small (fig. 2) and follows a bifurcation sequence of T, 2T, 4T period doubling, as sown in the diagram of fig. 3.

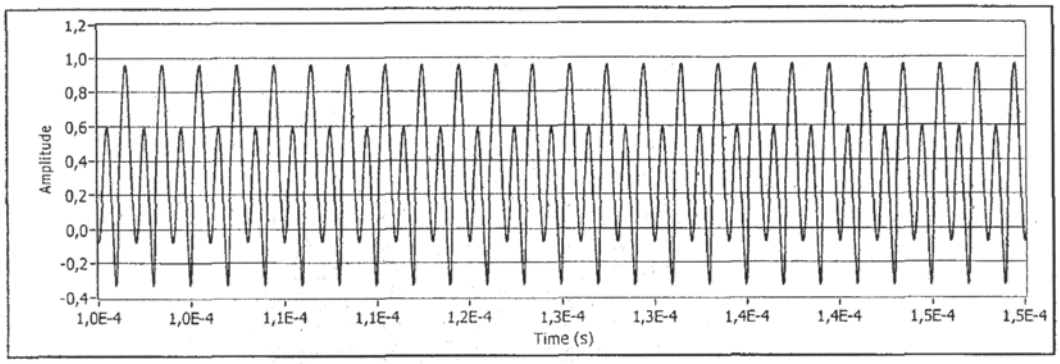

***Figure 2**: A period doubling for low amplitude external signal at $V_o=8V$ ($f_o=1MHz$).*

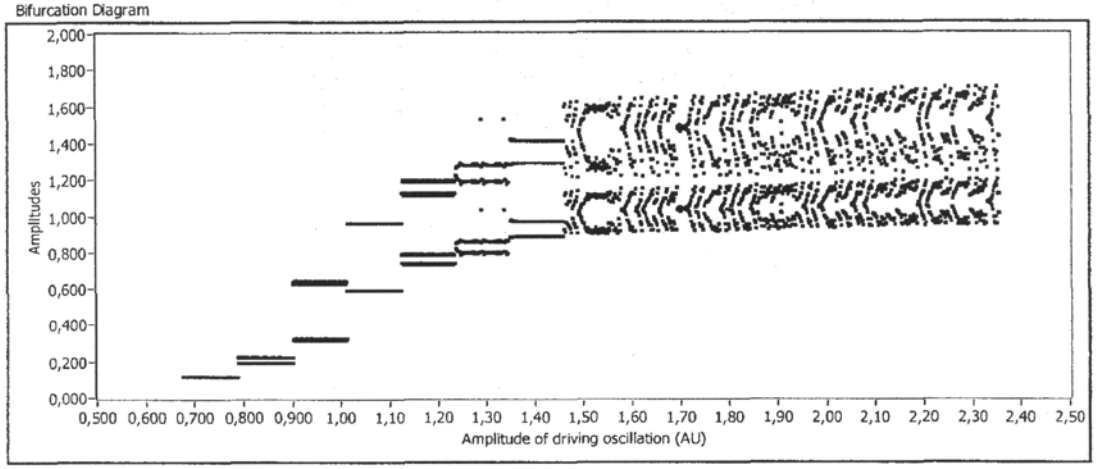

***Figure 3**: Bifurcation diagram with driving amplitude from 1 to 8 Volts ($f_o=1MHz$).*

For a critical driving amplitude (V_0=10.8 V) the system undergoes a characteristic bifurcation and a new resonant frequency appears, as shown in fig. 4. The new oscillation has a basic frequency of about 9.350 kHz, while its power spectrum is rich in higher harmonics.

By increasing further the amplitude of the external oscillation we observe an interesting nonlinear behavior with a number of periodic instants. In-between periodic instants we observe non-periodic waveforms which become denser in chaotic content as the driving amplitude increases. This behavior is shown in figs. 5 (a-f).

Periodic instants shown in figs. 6 (a-e) are characterized by a modulation of the external driving frequency of 1 MHz by peaks of lower frequency in the region 10 to 100 kHz (fig. 7). The fixed relationship between these two frequencies for each waveform corresponds to a frequency locking of two interacting oscillators. The periodicity of these waveforms holds within the resolution of the solutions produced for the given parameter values.

Before we proceed to analyze the data presented in this paragraph we shall discuss a raw model for the interpretation of the above nonlinear behavior.

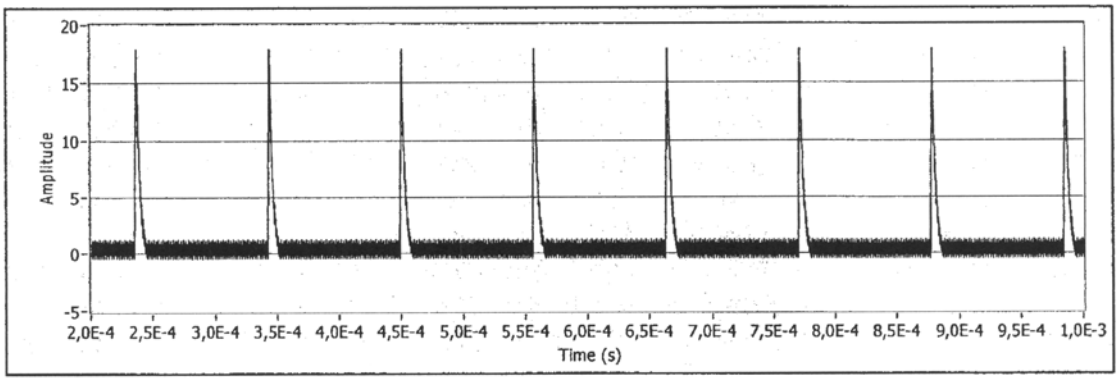

***Figure 4**: First appearance of a new low frequency signal for external driving at Vo=10.8V*

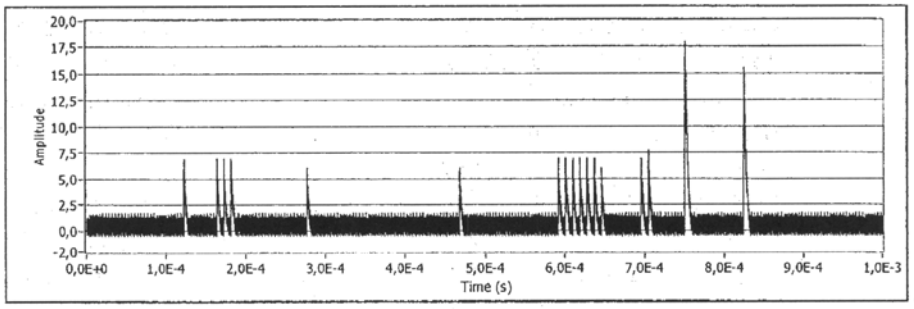

(f_o=1MHz)

(a) *V_0=13,75V*

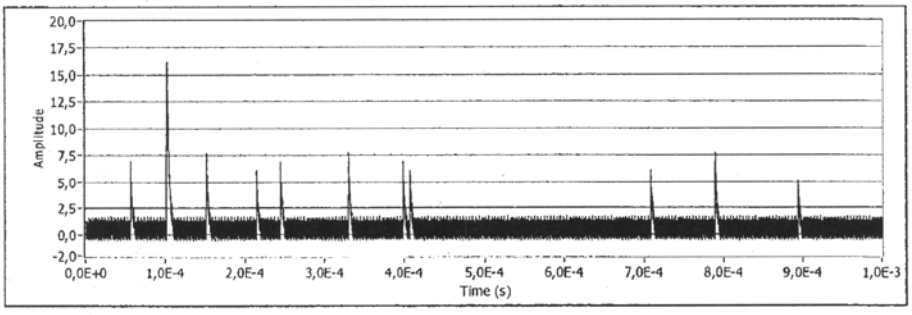

(b) *V_0=13,85V*

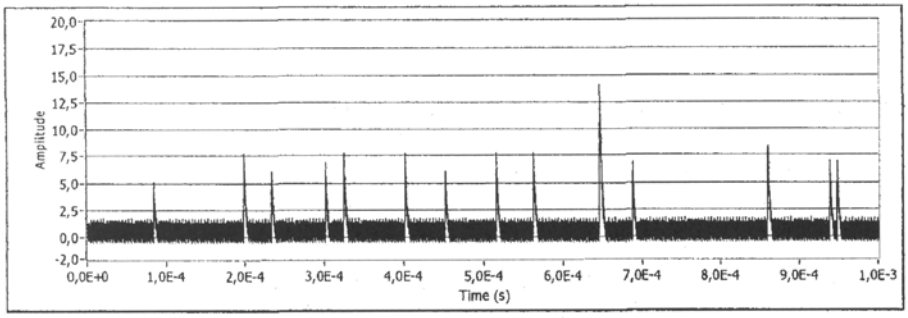

(c) V_0=13,9 V

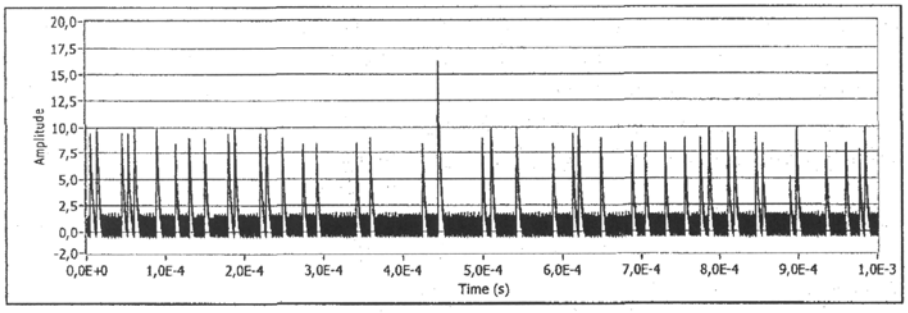

(d) V_0=14,9 V

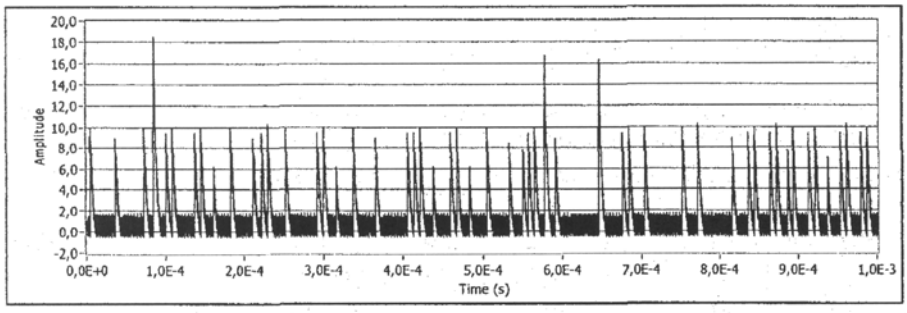

(e) V_0=15,05 V

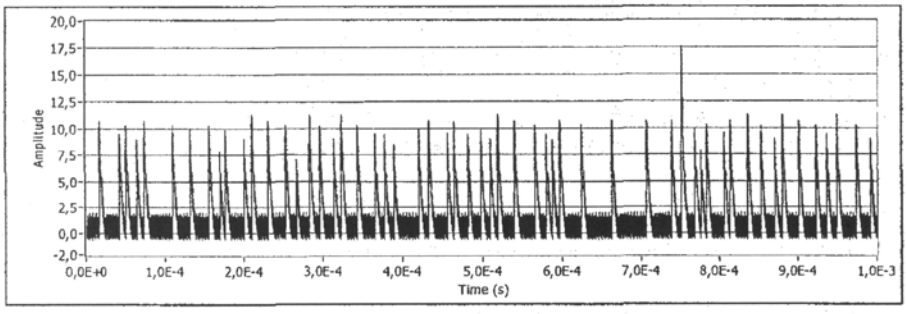

(f) V_0=16,3 V

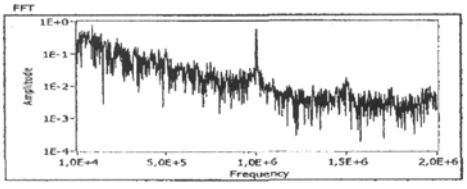

(g) *FFT of 5(f)*

Figure 5: *Non-periodic signals obtained between mode-locking instants. In fig.5(g) the FFT of 5(f) is shown.*

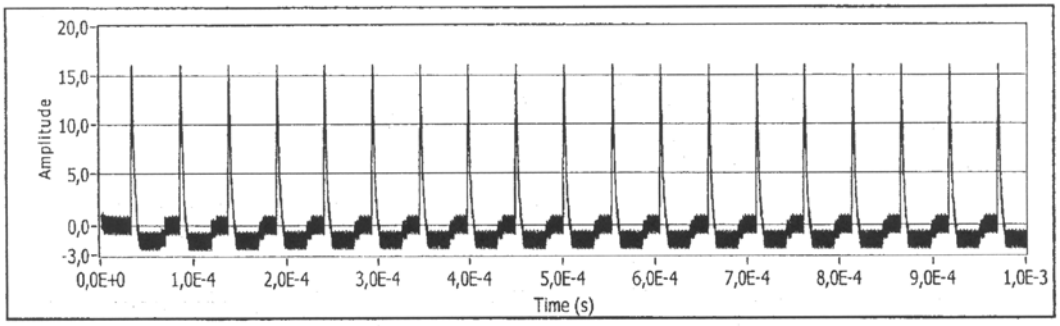

(a) V_0=11,556 V

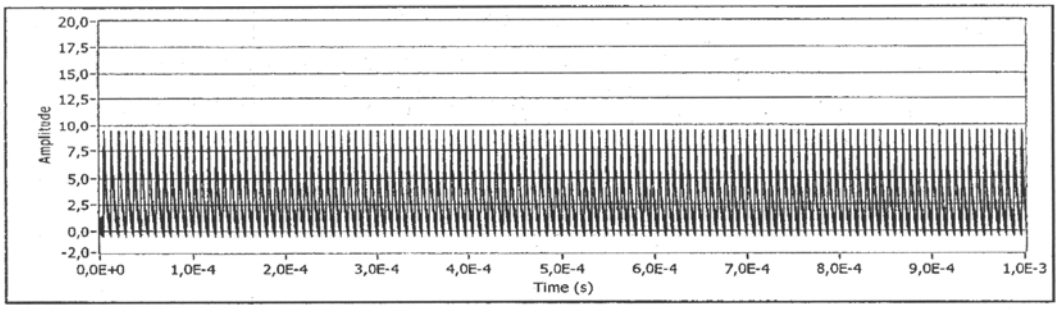

(b) V_0=14,5V

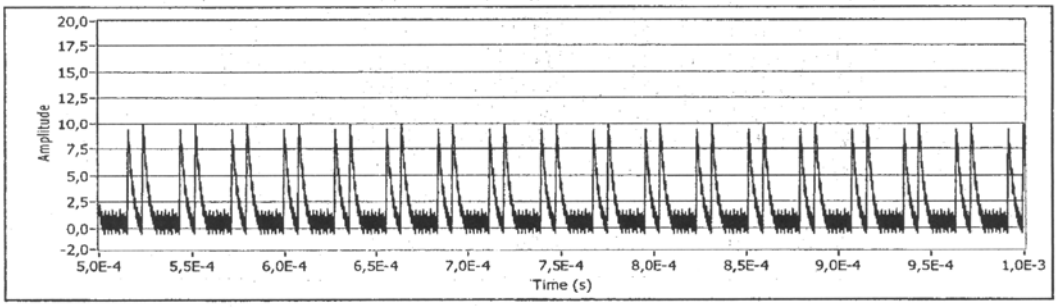

(c) V_0=15V

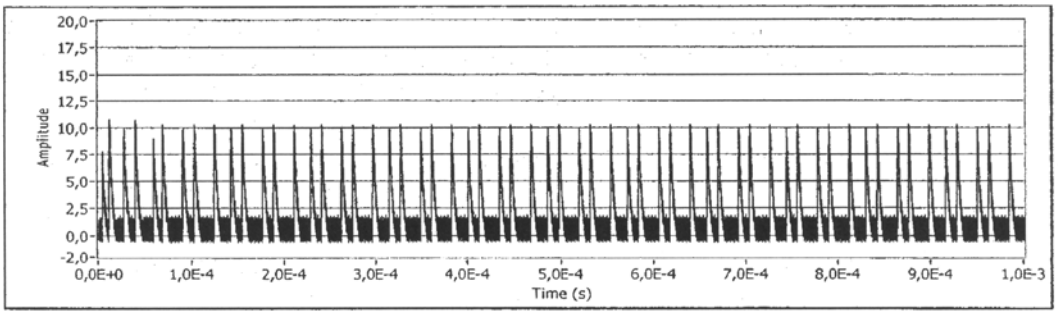

(d) V_0=16 V

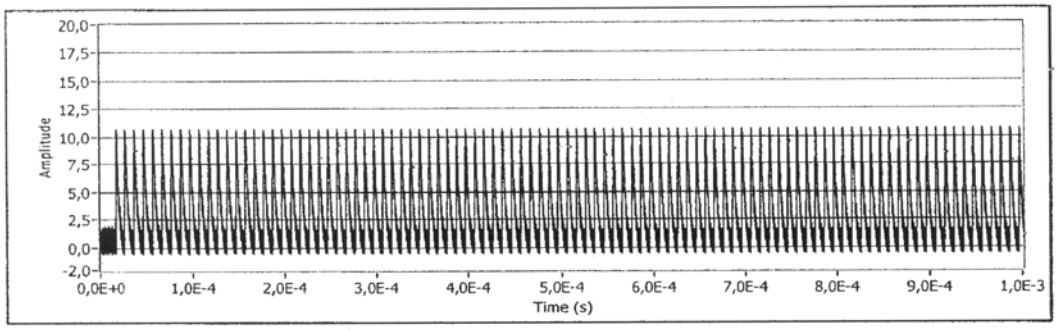

(e) V_0=17 V

Figure 6: *Periodic-like instants at various driving amplitudes*

III. Low frequency resonator model

To interpret the new resonance arising in the RLD circuit at low frequencies we need to take into account three different values of the diode capacitance. First of all in the voltage region $V>Vo$, a large diffusion capacitance, caused by diffused minority charge carriers during forward bias, dominates (Vo is the forward bias voltage drop across the diode). Secondly, the reverse bias capacitance which is lower than the diffusion one and is voltage dependent, dominates in the region of reverse bias, for most bias voltages. Both capacitances are included in all piecewise models discussed in the literature. In the present report we take into account a third capacitance, due to injected majority carriers at reverse bias breakdown. Its contribution to the total diode capacitance should only arise for large values of reverse bias or for alternating driving signals of large amplitude.

In this case, a new time-constant appears in the circuit, associated with the discharge of the injected majority carriers, into the external resistance R. This time-constant represents the recovery time required for the majority carriers to move back when the reverse voltage pulse is removed.

As the amplitude of the driving oscillation increases, the R-L-varactor circuit may respond like a resonance circuit of large capacitance and can tune in to some lower harmonic of the driving frequency. Low frequency content is present in the output signal measured on the external resistor, since the R-L-varactor circuit can respond like a nonlinear low-pass filter at high driving amplitudes. This way, resonances at two frequencies can be established, as the resonating qth lower harmonic of the driving frequency locks in with the base frequency of the driving signal.

Since resonance at a lower harmonic is associated with breakdown capacitance, it produces narrow reverse bias pulses that lead to breakdown and to reverse current injection through the diode. In response, a low frequency voltage peak appears on the resistor R, followed by a short discharging effect.

IV. Sine-circle map computations

In order to gain insight of the system's behaviour, we use the sine-circle map above criticality. The sine-circle map includes several universal properties of the nonlinear dynamics of interacting oscillators, but admittedly it provides a limited description of the chaotic regime of a real system, where trajectories require at least a three-dimensional state-space. In such cases the Poincaré section is a two-dimensional map. However, one-dimensional maps like the sine-circle map have been found to provide useful descriptions of frequency locking and of the transition from quasi-periodicity to chaos in real systems [10].

The sine-circle map is a nonlinear map function with the nonlinearity taking the form of a sine function [11]:

$$\theta_{n+1} = \theta_n + \Omega - \frac{K}{2\pi}\sin(2\pi\theta_n) \bmod 1 \quad (1)$$

The parameter K (with K>0) is a measure of the strength of the nonlinearity and Ω is the frequency ratio of the interacting oscillators.

As is known the sine-circle map for K<1 produces quasi-periodic trajectories on a two-dimensional torus, when the frequencies f_1 and f_2 are incommensurate ($\Omega = f_1/f_2$ is irrational) and frequency-locked behaviour with commensurate frequencies (Ω is a rational number). In the last case the resulting motion is periodic and the trajectory closes on itself on a torus surface.

For K>1 the map becomes non-invertible and the resulting folding of trajectories may lead to chaotic behavior. Large values of K mean stronger coupling between the oscillators and such values are closely associated with large amplitudes of the driving signals. In this regime (K>1) the sine-circle map produces either mode-locking with periodic trajectories or chaos.

We should note that real oscillatory systems in their transition to chaos may present a bifurcation from two-frequency mode-locking or quasi-periodicity to three-frequency quasi-periodicity on a three-dimensional torus, according to the Ruelle-Takens-Newhouse scenario [12]. Small changes of the system convert the motion from a quasi-periodic three-frequency flow to a chaotic flow. However, stronger couplings between the oscillators may result in a transition from two-frequency quasi-periodicity directly to chaos.

Given the above differences between the sine-circle map and a real system with two interacting oscillators, we present our circle-map computations in the region where K>1 (2.8<K<3.7) with a frequency ratio Ω=0.3. Our purpose is to show that there is a qualitative agreement between our simulated response shown in figs. 5, 6 and the computed trajectories produced with the map function. Fig. 7a shows the first iteration of the map function plotted versus angle θ. In this figure θ_{n+1} is plotted against θ_n with Ω=0.3 and K=2.8. The super-critical condition results in non-invertibility due to the local maximum.

In the lower K region (K<3.3) the trajectories are confined in the lower left side of the map diagram and follow a bifurcation sequence leading to period 4T. Fig.7c shows the trajectory evolution for successive iterations, where period 4 is manifested. Increasing the K value a discontinuity of the iterative function appears (fig. 7c) and trajectories escape into a new region of the phase space. Large amplitude peaks become denser as trajectories flow

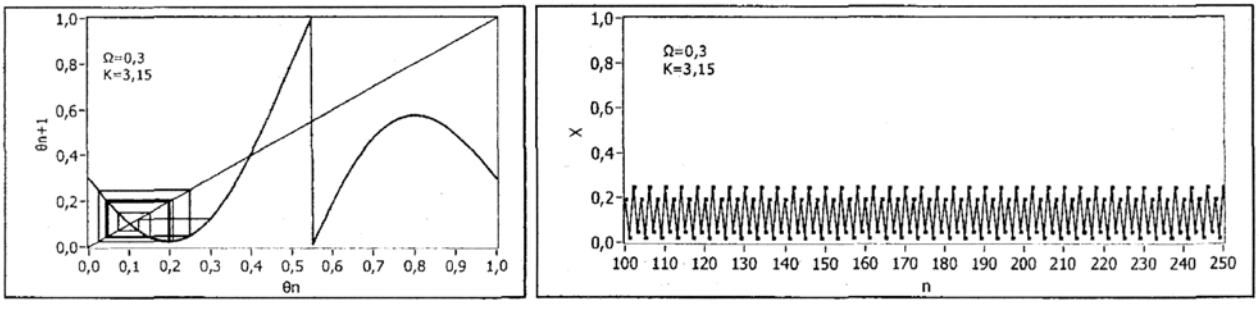

a b

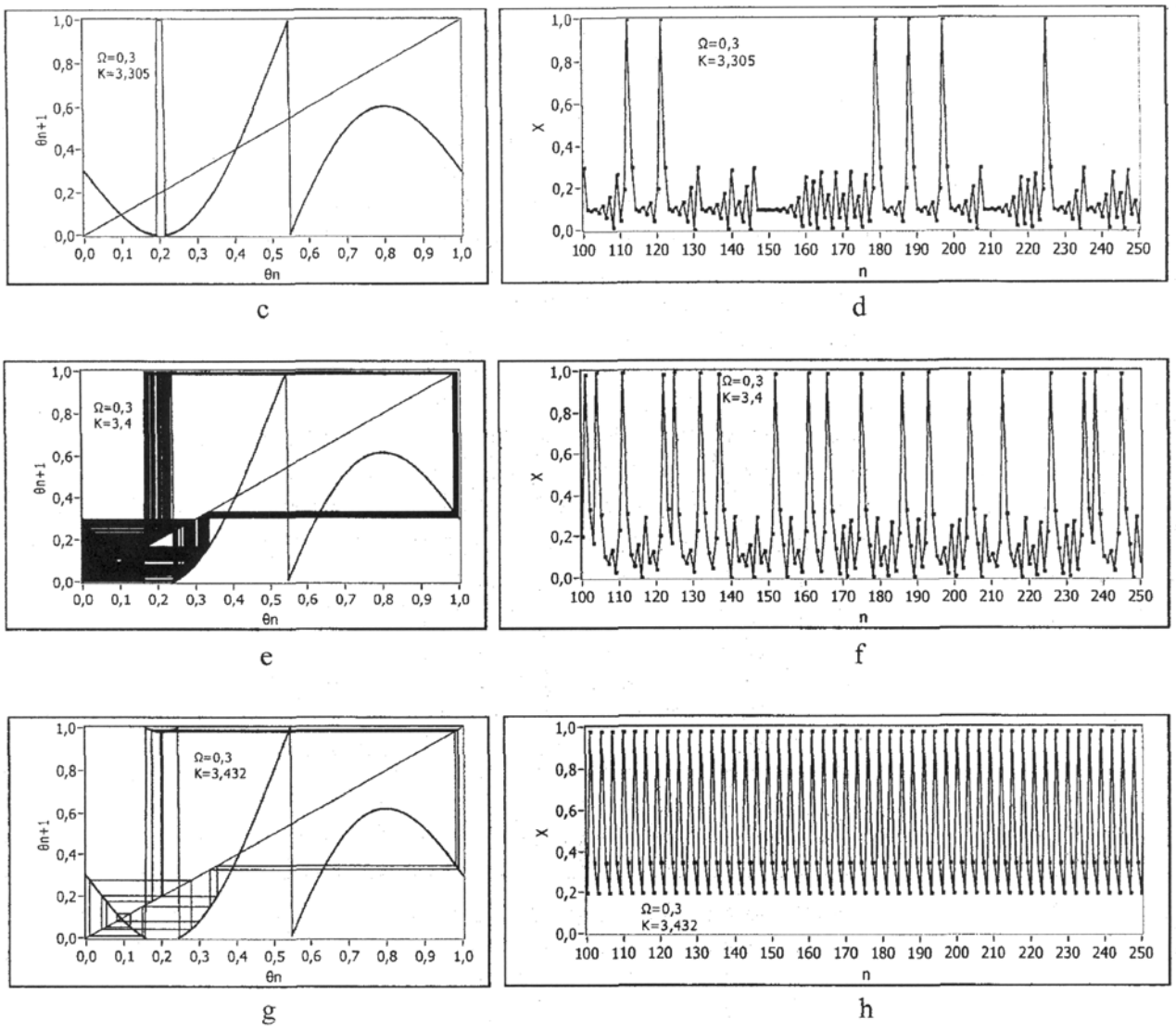

***Figure** 7: On the left, the circle map function is plotted for increasing values of K above criticality (a,c,e,g). The diagonal y=x and the graphic iteration scheme is also shown. On the light, the responding trajectory evolutions (b,d,f,h).*

back and forth, between the regions of the state phase, in an intermittency-like effect, until a new periodicity with unity amplitude sets in (fig. 7h).

These computations are in qualitative agreement with the waveforms produced by the simulation of the R-L-Varactor circuit, as shown in fig. 5 of the previous section. The above study identifies the general frame of interpretation of our signals to be that of the motion on a torus surface resulting in frequency locking and possibly in quasi-periodic motion and chaos.

V. Evaluation of periodic-like waveforms

A bifurcation to a high amplitude oscillation occurs at V_0=10.8V (fig. 4). Other periodic instants occur at V_0=11.556V; 14.500V; 16.000V; 17.000V. For such signals, the trajectories escape from the original low-amplitude oscillation at 1MHz and reside on the surfaces of well defined tori. A characteristic example is the waveform of fig. 6b (V_0=14.5V), which

represents mode-locking with a frequency ratio $f_0/f = 8.0$, where f_0 is the driving frequency of 1MHz and f is the low frequency of the oscillating response on the external resistor R. According to FFT spectra, this frequency is 125 KHz.

The Poincaré section of this waveform was constructed by picking out points at intervals that represent the recurrence time T, according to the Takens-Crutchfield technique [13]. In this case, the Poincaré cross-section corresponds to I[(n+1)T] vs I(nT) plot. As is shown in Fig. 8a the Poincaré cross-section for the waveform at V_0=14.5V consists of eight points at which the trajectories meet the Poincaré plane. This means that the trajectory pernes eight times before it completes a full turn around the torus (corresponding to a winding number w=8). On the other hand, this rational frequency ratio may be dictated by the resolution of the numerical solution, chosen by the simulator program in order to calculate the response. A small change in the parameters involved, might render the frequencies incommensurate and the motion quasi-periodic and for this reason we would rather refer to this group of signals as "periodic-like" waveforms.

In fig. 8b we present the Poincaré section of the signal obtained at V_0=10.8V (fig. 4), together with the cross-section shown in fig. 8a. The pattern is reminiscent of the cross-section of a nested tori structure.

Fig 9 presents the Poincaré cross-section corresponding to other periodic-like signals, at higher driving amplitudes. It is interesting to note the bifurcation or breakup of the original tori into smaller "ellipses", like in a period-doubling sequence.

Fig. 10 shows the Poincaré cross-section corresponding to the waveform in fig. 5f (V_0=16.3V), which is typical of non-periodic waveforms, at high driving amplitudes. This cross-section manifests a characteristic scattering while it preserves a shape similar to the original ellipse.

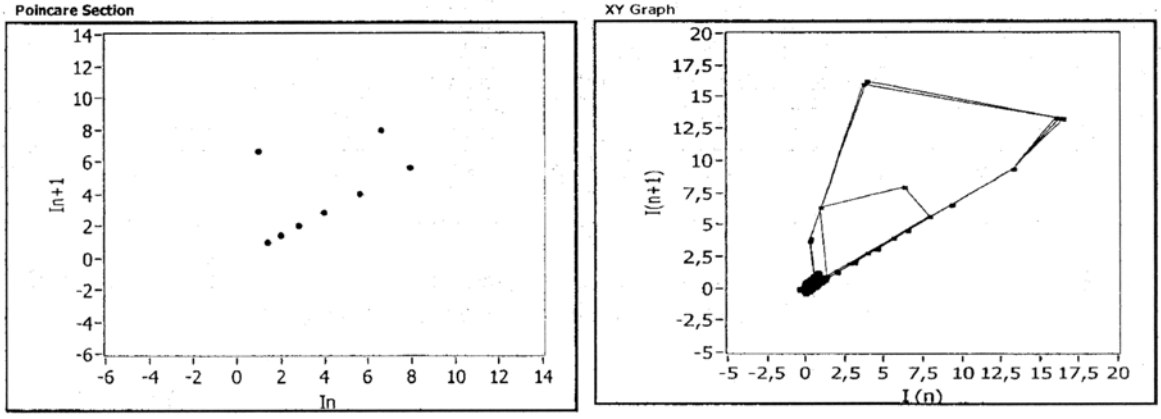

(a) (b)

Figure 8: *Poincaré cross-sections of periodic waveforms. In (a) a frequency ratio f_0/f=8.0 is depicted (V_0=14.5V) and in (b) a nested tori structure corresponds to oscillations with different resonant peak amplitudes (driving amplitudes were V_0=14.5V and V_0=10.8V).*

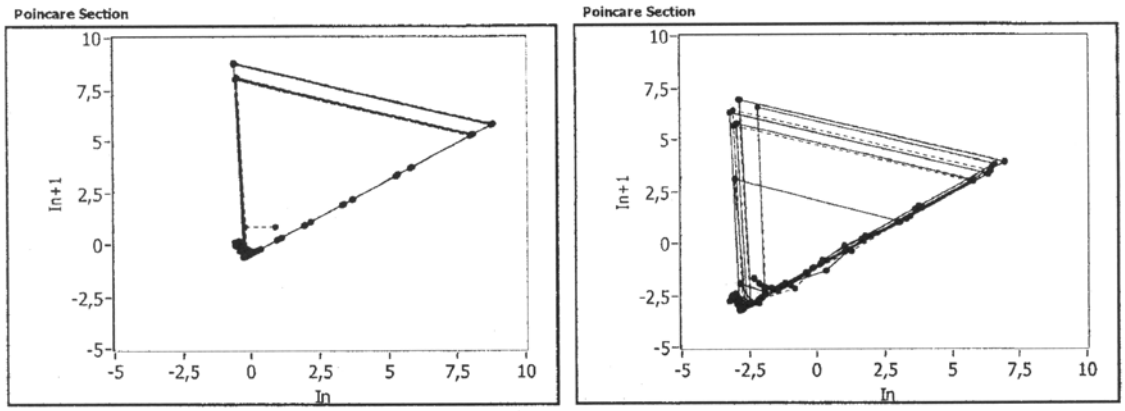

Figure 9: *Tori breakup at higher driving voltages: (a) V_0=15V, (b) V_0=15.1V*

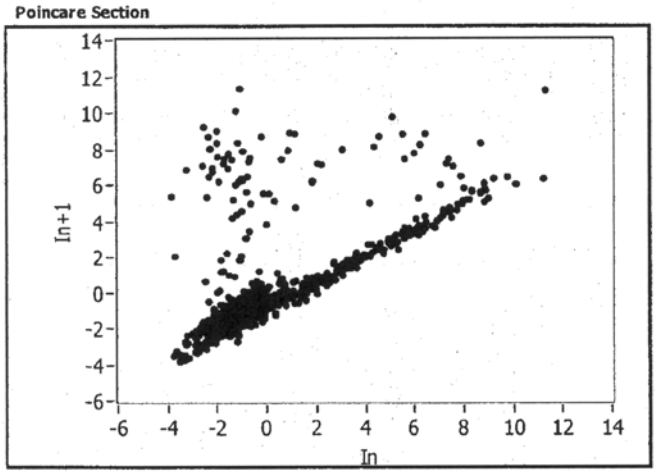

Figure 10: *Poincaré cross-section of the non-periodic waveform obtained with driving amplitude V_0=16.3V (see waveform in fig 5f).*

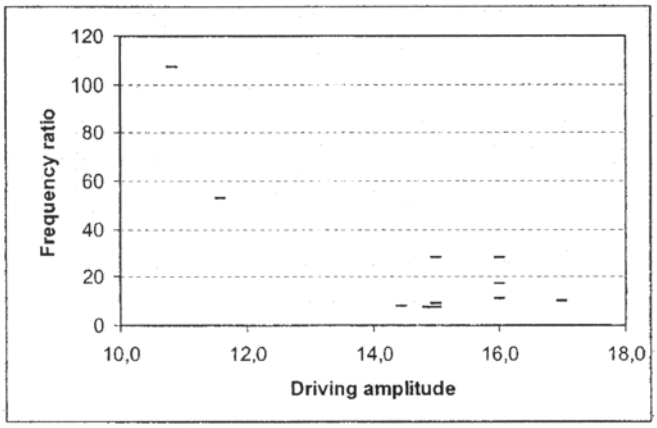

Figure 11*: Frequency ratio of periodic waveforms as a function of driving amplitudes. Multiple ratios correspond to period-doubling.*

Finally, fig.11 presents an analogy with the devil's staircase, its steps denoting frequency-locking instants, with the frequency ratio on the y-axis and driving amplitude on the x-axis. Between mode-locking are the chaotic intervals. Multiple lines represent torus breakup.

Frequency-locked instants with high ratios are unstable and vanish easily, while tori with low ratios persist for larger amplitude intervals.

VI. Evaluation of non-periodic waveforms

The power spectra of waveforms obtained in-between periodic-like instants exhibit a continuous background that increases with increasing driving amplitude. The driving frequency at 1 MHz and a bunch of sharp lines in the overall spectrum are also present. An example is given in fig. 5f where the FFT spectrum of the waveform at V_0=16.3V is shown. This is the waveform that corresponds to the Poincaré cross-section of fig. 10. We evaluate the chaotic content of this time-series by the Grassberger and Procaccia box counting technique [14,15]. For this purpose the value of the correlation integral C_l is computed for different instances l. The result is shown in fig. 12a where different curves correspond to different embedding dimensions. The state-space is reproduced by the displaced vectors technique using an appropriate delay time τ, obtained by the first nullification of the autocorrelation function. In a logarithmic plot the slopes of the curves in fig. 12 correspond to the reconstructed state-space dimension. With increasing number of displaced vectors, this slope tends to a limit value corresponding to the correlation dimension of the chaotic attractor. As shown in the slope diagram of fig. 12b the correlation dimension of our chaotic attractor is 3.3. This number means that the attractor needs a minimum embedding dimension m=4 while a three-dimensional torus is not enough to embed the trajectories.

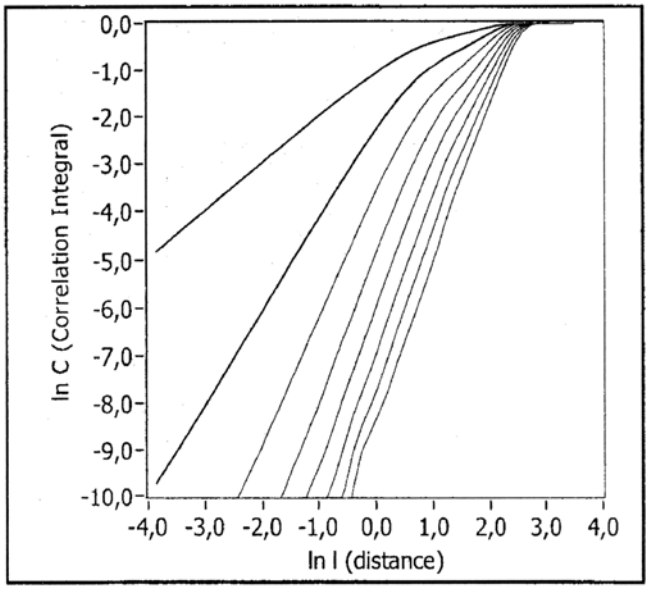

Figure12(a): *Correlation integral as a function of distance in a state-space of increasing dimensions according to the Grassberger and Procaccia box-counting method*

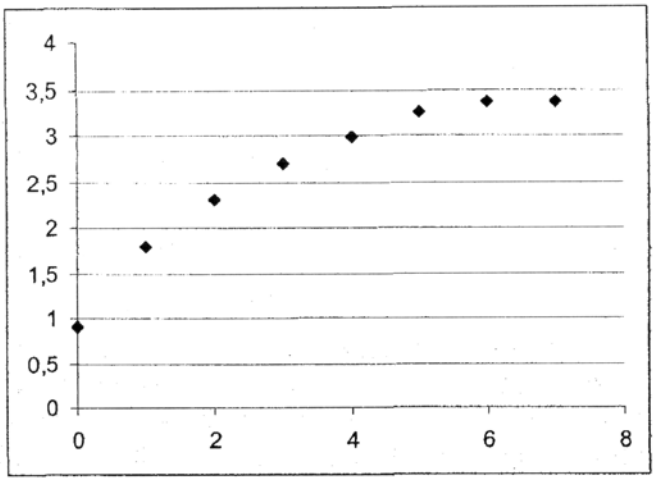

Figure 12(b): *Slopes of the curves in fig. 12a with increasing space dimension. The limit 3.3 represents the fractal dimension of the chaotic attractor*

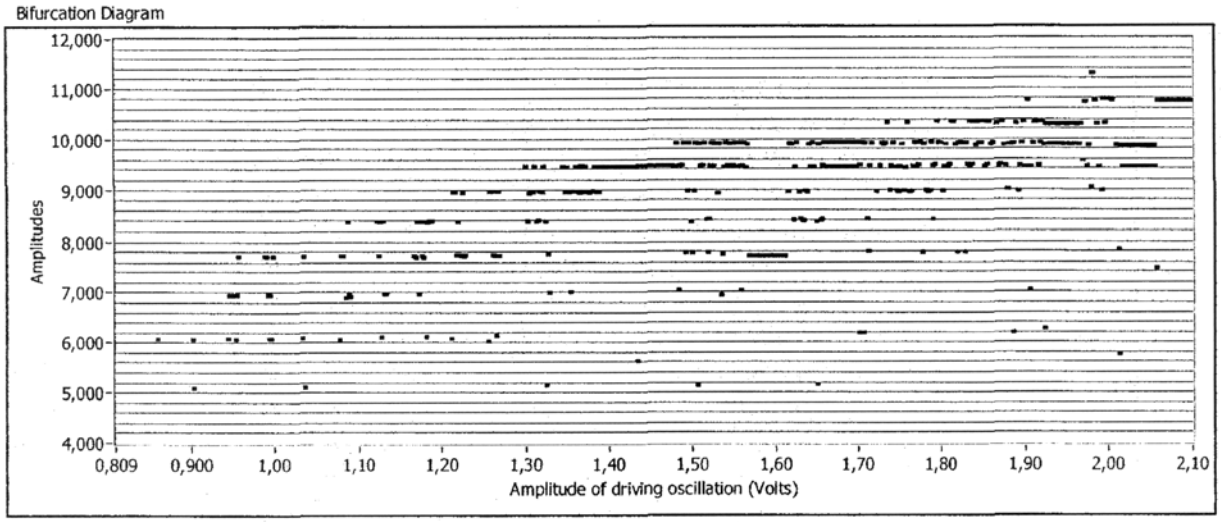

Figure 13: *Amplitudes of the resonant peaks in both periodic and non-periodic waveforms with driving amplitudes between 10 and 17V (x-axis in A.U.)*

VII. Discussion

The amplitudes of the simulated waveforms fall into well defined groups. Low frequency signals are characterized by high amplitude peaks, while higher frequency signals oscillate with peak amplitudes of about 10V. Non-periodic signals appear for driving voltages above V_0=13V and are easily monitored, in contrast with periodic trajectories which are observed at very specific driving voltages and are easily lost with a small parameter change.

Peak amplitudes of the non-periodic waveforms fall again into well-defined groups – as if trajectories are confined in specific regions in the phase space. Although the tori associated with periodic trajectories dissolve easily, it seems that non-periodic trajectories are still characterized by some organization, probably provided by surviving tori.

In Fig. 13, peak amplitudes for a large number of waveforms, both periodic and chaotic, are shown. The most interesting region between 5 and 11 Volts was enlarged. Amplitudes seem to take specific values, probably corresponding to a variety of two-dimensional tori in the four-dimensional state-space.

Acknoledgements

This work was supported by the NATO ICS EAP.CLG 981947 project.

References

[1] E. R. Hunt, Phys. Rev. Lett., vol. 49, 1054 (1982)

[2] J. Testa, J. Perez and C. Jeffries, Phys. Rev. Lett., vol. 49, 1055 (1982)

[3] R. W. Rollins and E. R. Hunt, Phys. Rev. Lett., vol. 49, 1295 (1982)

[4] T. Matsumoto, L. O. Chua, S. Tanaka, Phys. Rev. A vol. 30, 1155 (1984)

[5] D.S. Brorson, D. Dewey and P.S. Linsay, Phys. Rev. A, vol. 28. 1201 (1983)

[6] T. Klinger, W. Meyer-Isle and W. Lauterborn, Phys. Lett., vol. 101A, 371 (1984)

[7] R. Van Buskirk and C. Jeffries, Phys. Rev. A vol. 31, 3332 (1985)

[8] Z. Su, R.W. Rollins, and E.R. Hunt, Phys. Rev. A, vol. 40, 2698 (1989)

[9] Renato Mariz de Moraes and Steven M. Anlage, Phys. Rev. E Vol. 68, 026201 (2003)

[10] Heins G. Schuster, "Deterministic Chaos: an introduction", VHC Verlagsgesellschaft mbH, Weinheim, 1989, p. 145.

[11] Rober C. Hilborn, "Chaos and nonlinear dynamics: an introduction for scientists and engineers", Oxford University Press, New York, 1994, p. 263.

[12] S. Newhouse, D. Ruelle, and F. Takens Commun. Math. Phys. Vol. 64, 35 (1978)

[13] J. Peinke, J. Parisi, O.E. Rössler, R. Stoop, "Encounter with Chaos: Self organized Hierarchical complexity in Semiconductor Experiments", Springer-Verlag, 1992, p. 85.

[14] P. Grassberger, I. Procaccia, "Measuring the strangeness of trange attractors", *Physica D,* 1983, 9, p. 189.

[15] P. Grassberger, I. Procaccia, [1983] "Estimation of the Kolmogorov entropy from a chaotic signal". *Phys. Rev. A*, 1983, 28, pp.2591-2593